

THE RULES FOR THE LATTICE ROTATION ACCOMPANYING SLIP AS DERIVED FROM A SELF-CONSISTENT MODEL

R.A. LEBENSOHN^a and T. LEFFERS^{b,*}

^a*IFIR (UNR-CONICET), 27de Febrero 210 Bis, 2000 Rosario, Argentina;* ^b*Materials Research Department, Risø National Laboratory, P.O. Box 49, DK-4000 Roskilde, Denmark*

(Received 29 July 1998; In final form 12 November 1998)

The rules for the lattice rotation during rolling (plane strain) deformation of fcc polycrystals are studied with a viscoplastic self-consistent model. Very high values of the rate-sensitivity exponent are used in order to establish Sachs-type conditions with large local deviations from the macroscopic strain. The lattice rotation depends on the grain shape. For equiaxed grains the lattice rotation follows the MA rule, which is the one normally used in solid mechanics. For elongated and flat grains the lattice rotation follows a different rule, the PSA rule. In the standard version the model performs a transition from MA to PSA with increasing strain. There is a very clear difference between the textures resulting from the two different rules. MA leads to a copper-type texture, and PSA leads to a brass-type texture.

Keywords: Lattice rotation; Rolling texture; Grain shape; Viscoplastic self-consistent model

INTRODUCTION

Already Hosford (1977) pointed at the ambiguity in the calculation of the lattice rotation corresponding to a specific slip activity in a grain (a crystallite) – an ambiguity which has nothing to do with the “Taylor ambiguity” (e.g. Leffers *et al.*, 1988) expressing an uncertainty in the selection of slip systems. More recently the problem has been discussed by Kocks and Chandra (1982) and Tiem *et al.* (1986). Hosford pointed

* Corresponding author.

at three different sets of rules for the calculation of the lattice rotation: "Schmid tension analysis", "Taylor compression analysis" and "mathematical analysis". The first and the second are identical to the rules for the lattice rotation in single crystals subjected to tension and compression, respectively. The third calculates the lattice rotation from the skewsymmetric component of the plastic distortion; it is the one normally used in solid mechanics (e.g. Kocks *et al.*, 1998). Recently it has been demonstrated that plastic deformation with special microstructural conditions may require specific rotation rules adjusted to the specific microstructure, e.g. Leffers (1994), Lebensohn and Canova (1997) and Bolmaro *et al.* (1997).

The present authors (Leffers and Lebensohn, 1996) have demonstrated the effect of the choice of rotation rule on the simulated rolling texture of fcc materials. In their work, the Schmid tension analysis and the Taylor compression analysis were combined to "plane-strain analysis" (PSA). PSA infers that a string of material originally oriented along the rolling direction maintains its orientation and a plate of material originally oriented parallel to the rolling plane also maintains its orientation. PSA is identical to the lattice rotation rule for single crystals subjected to plane strain in a channel-die experiment (but channel-die deformation imposes special constraints which are not part of PSA). The mathematical analysis (MA) is independent of the deformation mode (tension/compression/plane strain). The lattice rotations according to MA and PSA are sketched in Fig. 1 (taken from Leffers and Lebensohn (1996)). An alternative illustration of the two types of lattice rotation has been presented by Van Houtte (1996), who is working with problems closely related to those dealt with in the present work (in Van Houtte's terminology $R = 0$ and $R = 1$ corresponds to MA and PSA, respectively).

For the Sachs model and the modified Sachs model (Sachs, 1928; Pedersen and Leffers, 1987) the rotation rule turned out to have a decisive effect on the simulated texture: PSA led to a brass-type simulated texture while MA led to a copper-type simulated texture. For the relaxed-constraint Taylor model (in the "pancake" mode, e.g. Van Houtte, 1981) there was a certain, not very pronounced, difference between the textures simulated with PSA and MA. For the full-constraint Taylor model (Taylor, 1938) the textures simulated with PSA and MA were identical – as they should be theoretically, e.g. Van Houtte (1996) and Leffers and Lebensohn (1996).

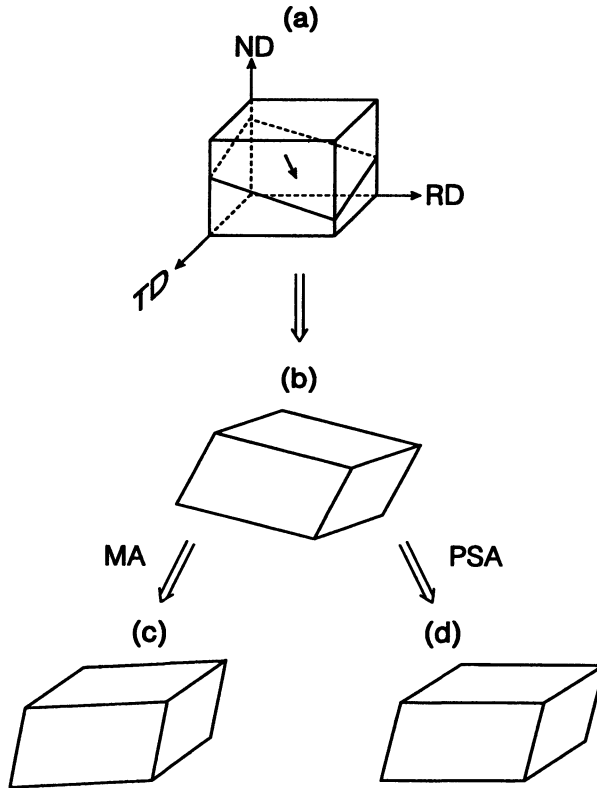


FIGURE 1 Sketch of the lattice rotation according to MA and to PSA; (a) before slip, (b) after slip, before lattice rotation, (c) after slip and lattice rotation according to MA, (d) after slip and lattice rotation according to PSA. In (c) the parallelepiped has no simple orientation relation to the axes of the sample coordinate system, whereas in (d) the parallelepiped has four edges parallel to the rolling direction and two faces parallel to the rolling plane. Slip plane and slip direction are indicated in (a).

As pointed out by Hosford, the logical choice of rotation rule is linked to the shape of the grains: MA is the logical choice for equiaxed grains whereas, for rolling deformation, PSA is the logical choice for the flattened and elongated grains at large strains. In various versions of the self-consistent model, e.g. Tiem *et al.* (1986) and Lebensohn and Tomé (1993), the grain shape enters explicitly in the calculation of the lattice rotation. In the present work we demonstrate, for fcc polycrystals, how such models (in this case that of Lebensohn and Tomé) infer a change from MA to PSA with increasing strain (increasing deviation from

equiaxed grains), and we discuss the basic assumptions behind the calculation of the lattice rotation in these models. We also discuss the reasons why one has to deal with non-Taylor models – and hence with the different rules for the calculation of the lattice rotation.

THE SELF-CONSISTENT MODEL

Self-consistent texture calculations were made with a viscoplastic self-consistent model (VPSC) (Lebensohn and Tomé, 1993). The VPSC model allows each grain to deform and rotate according to a local velocity gradient that can be different from the macroscopic velocity gradient. How much the local behaviour differs from the overall behaviour is determined by the strength of the interaction between the individual grain, considered as an ellipsoidal inclusion, and its surroundings, considered as a homogeneous equivalent medium (HEM) with behaviour and properties derived as the average for the whole polycrystal. The interaction equation can be expressed as:

$$\tilde{\varepsilon}_{ij} = -\tilde{M}_{ijkl}\tilde{\sigma}'_{kl}. \quad (1)$$

In (1) $\tilde{\varepsilon}_{ij}$ and $\tilde{\sigma}'_{kl}$ are the local deviations – relative to the macroscopic state – of strain rate and deviatoric stress, respectively, and \tilde{M}_{ijkl} is the interaction tensor defined as:

$$\tilde{M}_{ijkl} = n(I - S)_{ijmn}^{-1} S_{mnpq} M_{pqkl} \quad (2)$$

where n is the rate sensitivity exponent and I , S and M are the symmetric identity tensor, the viscoplastic Eshelby tensor and the secant viscoplastic compliance tensor. It should be noticed that a high value of the rate sensitivity exponent n corresponds to a low degree of rate sensitivity, e.g. Kocks *et al.* (1998).

After each deformation step, the local strain and rotation represent a compromise between what the individual ellipsoidal grain would have done if it were unconstrained and what the polycrystal is doing as a whole. The total crystallographic rotation rate of a grain, calculated with a self-consistent model, can be expressed as:

$$\dot{\omega}_{ij} = \dot{\Omega}_{ij} + \tilde{\omega}_{ij} - \dot{\omega}_{ij}^{\text{pl}}. \quad (3)$$

Here $\dot{\Omega}_{ij}$ is the macroscopic rotation rate tensor, and $\dot{\omega}_{ij}^{\text{pl}}$ is the rotation rate associated with plastic deformation:

$$\dot{\omega}_{ij}^{\text{pl}} = \sum_s \frac{1}{2} \left(n_i^s b_j^s - n_j^s b_i^s \right) \dot{\gamma}^s \quad (4)$$

where the summation includes all the active slip systems and \bar{n}^s , \bar{b}^s and $\dot{\gamma}^s$ are the normal ($\langle 111 \rangle$) and Burgers ($\langle 110 \rangle$) vectors and the shear rate of systems s . $\tilde{\omega}_{ij}$ is an additional rotation rate associated with grain morphology given by:

$$\tilde{\omega}_{ij} = \prod_{ijkl} S_{klmn}^{-1} \tilde{\epsilon}_{mn} \quad (5)$$

where Π is the skewsymmetric Eshelby tensor for rotation (Lebensohn and Tomé, 1993). Both S and Π depend on the anisotropy of the HEM and on grain shape. As a consequence, the relative weight of $\tilde{\omega}_{ij}$ in Eq. (3) increases with increasing flatness and elongation of the grains. Thus, the strain dependence of the rotation rules comes via $\tilde{\omega}_{ij}$.

Within the VPSC scheme, the principal axis of the ellipsoidal grains will try to keep as aligned as possible with the principal directions of the sheet. Since an arbitrary strain applied to an ellipsoid changes the orientation of its principal axis, the term $\tilde{\omega}_{ij}$ can be regarded as an supplementary rotation that tends to realign the new ellipsoid axes with the macroscopic principal directions.

As it can be seen from Eqs. (1) and (2), the assumption of a high value of the rate sensitivity exponent n (a low degree of rate sensitivity) can make the VPSC model approach a Sachs type model, i.e. we can produce calculated textures derived from a slip pattern which is similar to that of the Sachs/modified Sachs model used by Leffers and Lebensohn (1996). Consequently, using a sufficiently high value of n (in the present case $n = 47$), we can compare the lattice rotations and the texture evolution prescribed by VPSC with those corresponding to PSA and MA in the work of Leffers and Lebensohn.

For the comparison of VPSC with PSA we determine, after a given deformation increment, the updated orientations of a string of material originally oriented in the rolling direction and of a plate of material originally oriented in the rolling plane. The coordinates in sample axes

of a vector \bar{v} after a deformation increment (i) are updated as:

$$v_i^{(i)} = a_{ij}^{(i)} a_{kj}^{(i-1)} (I + e^{pl})_{kl} v_l^{(i-1)} \quad (6)$$

where a_{ij} is the transformation matrix from crystal to sample, I is the symmetric second order identity tensor, e^{pl} is the plastic distortion tensor and the indices (i - 1) and (i) refer to coordinates before and after the deformation step, respectively. If \bar{r} and \bar{n} are vectors parallel to the rolling direction and perpendicular to the rolling plane, respectively, the incremental (inc) and integrated (int) RD and ND misorientations (reflecting deviations from PSA) for deformation increment (i) are defined as:

$$RD_{inc} = \langle \text{angle}(\bar{r}^{(i)}, \bar{r}^{(i-1)}) \rangle \quad (7)$$

$$RD_{int} = \langle \text{angle}(\bar{r}^{(i)}, \bar{r}^{(0)}) \rangle \quad (8)$$

$$ND_{inc} = \langle \text{angle}(\bar{n}^{(i)}, \bar{n}^{(i-1)}) \rangle \quad (9)$$

$$ND_{int} = \langle \text{angle}(\bar{n}^{(i)}, \bar{n}^{(0)}) \rangle \quad (10)$$

where $\langle \rangle$ expresses a weighted average over the whole set of grains.

For the comparison of VPSC with MA we refer to $\tilde{\omega}_{ij}$ in Eq. (3) which represents the deviation from MA. We express the deviation by the following parameters:

$$\text{average misorientation} = \langle \text{angle}(\underline{\omega}^{(i)}, \underline{\omega}^{pl(i)}) \rangle \quad (11)$$

$$\text{average relative modulus} = \left\langle \frac{|\tilde{\omega}^{(i)}|}{|\tilde{\omega}^{pl(i)}|} \right\rangle \quad (12)$$

where $\underline{\omega}^{(i)}$, $\underline{\omega}^{pl(i)}$ and $\tilde{\omega}^{(i)}$, $\tilde{\omega}^{pl(i)}$ are the pseudo-vectors associated with the corresponding skewsymmetric tensors. Since $\tilde{\Omega}_{ij} = 0$ in rolling, the first parameter is the average misorientation of the instantaneous rotation axis associated with VPSC and MA, respectively, while the second is an average of the normalized modulus of the extra term $\tilde{\omega}_{ij}$. The smaller these two parameters are, the smaller is the difference between VPSC and MA.

RESULTS

As it turns out, the VPSC model does not, even with n as high as 47, lead to a proper Sachs-type deformation pattern. At the early stage of deformation (with spherical grains) the average number of active slip systems in the grains is ~ 1.77 to be compared with an average number very close to 1.0 for Sachs. For practical computational reasons we cannot go to higher n values than ~ 47 . However, the strain in the individual grains deviates very significantly from the macroscopic strain, which means that the different rotation rules do give different rotations. After 1% strain the average local absolute deviation of the strain from the macroscopic strain (average for all grains and all strain components) is 0.27%, which is about the same as the 0.25% quoted for the Sachs model by Pedersen and Leffers (1987).

Figure 2 shows the development with strain of the four indicators of deviation from PSA defined in Eqs. (7)–(10). Three cases are considered: change in grain shape with strain starting with equiaxed grains (“updated”), permanently spherical grains (“spherical”) and permanently flat grains (“flat”). With updating the incremental ND and RD misorientations (Fig. 2(a) and (b)) very clearly show a development towards PSA (low incremental ND and RD misorientations) with increasing strain. For spherical grains the misorientations remain high – with minor variations due to texture formation. For flat grains the misorientations remain low.

Figure 3 shows the development with strain of the two indicators of deviation from MA defined in Eqs. (11) and (12) for the same three cases as above. With updating, there is a clear change away from the initial MA conditions (low modulus and low misorientation) with increasing strain. For spherical grains the deviations from MA remain low, and for flat grains they remain high – with fluctuations due to texture.

From Figs. 2(a), (b) and 3(a) the “transition point”, the strain where the lattice rotation is halfway between MA and PSA, may be estimated. The transition point is at a strain of ~ 0.5 .

Figure 4 shows the development of the five major texture components with strain for the three cases (updated, spherical, flat): the copper component $\{211\} \langle 111 \rangle$, the brass component $\{110\} \langle 112 \rangle$, the S component $\{123\} \langle 634 \rangle$, the Goss component $\{110\} \langle 001 \rangle$ and the cube

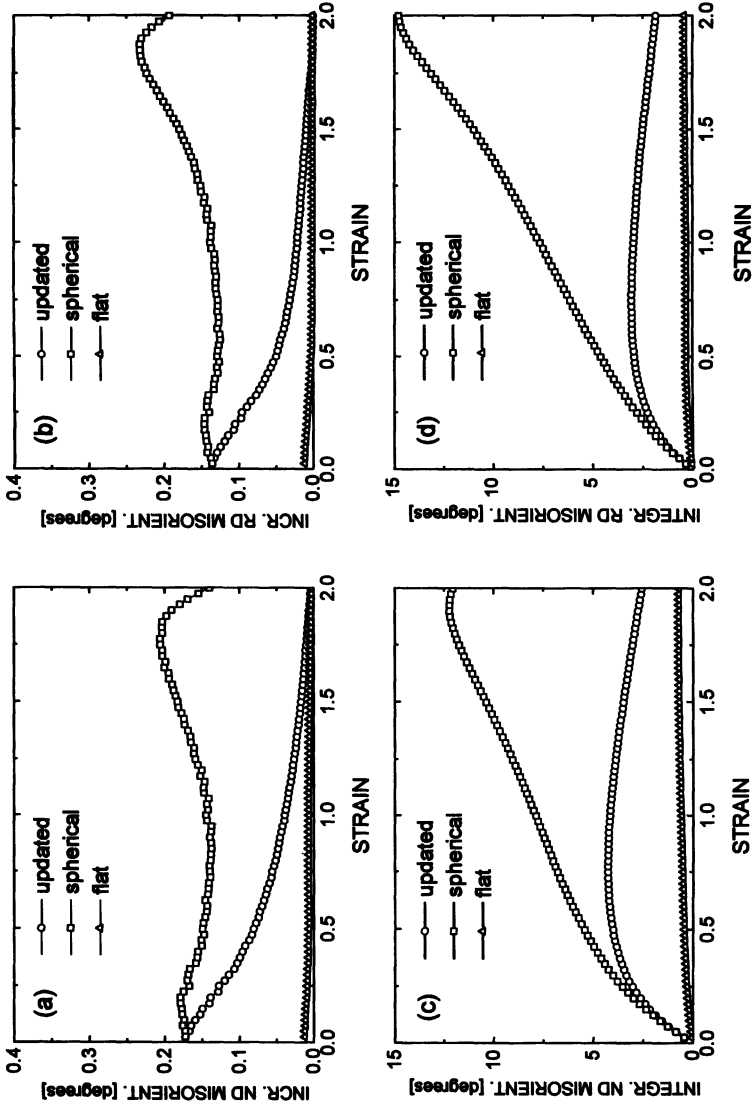


FIGURE 2. Development with strain (von Mises equivalent strain) of the four indicators of deviation from PSA: (a) incremental ND misorientation; (b) incremental RD misorientation; (c) integrated ND misorientation; (d) integrated RD misorientation. In (a) and (b) the unit along the y -axis is actually degrees per percent of strain.

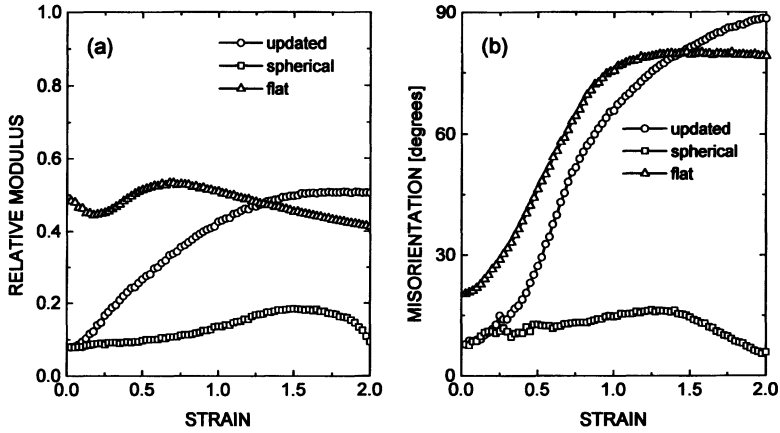


FIGURE 3 Development with strain of the two indicators of deviation from MA: (a) relative modulus; (b) misorientation.

component $\{100\} \langle 001 \rangle$. For all components orientations within 15° from the ideal orientation are included.

For permanently spherical grains (which should correspond to MA) the final texture is an extreme copper-type texture with a strong predominance of the copper component. For permanently flat grains (which should correspond to PSA) the final texture is a brass-type texture with a very strong brass component, a fairly strong S component and a significant Goss component. For updating, the development of the different texture components is not just somewhere between that for spherical grains and that for flat grains. At a strain of 0.5, which corresponds to the transition strain estimated above, the copper component is weaker for updating than for spherical grains and flat grains.

Figure 5 shows the calculated $\{111\}$ and $\{200\}$ pole figures for a strain of 0.5. Again one notices that updating does not lead to a texture between the textures for spherical and flat grains. The pole figures for updating are brass-type pole figures like those for flat grains (the $\{111\}$ pole figure for updating actually comes closer to the brass-type texture than that for flat grains). For permanently spherical grains (MA) and permanently flat grains (PSA) the pole figures qualitatively agree with those presented by Leffers and Lebensohn (1996): copper-type for MA and brass-type for PSA.

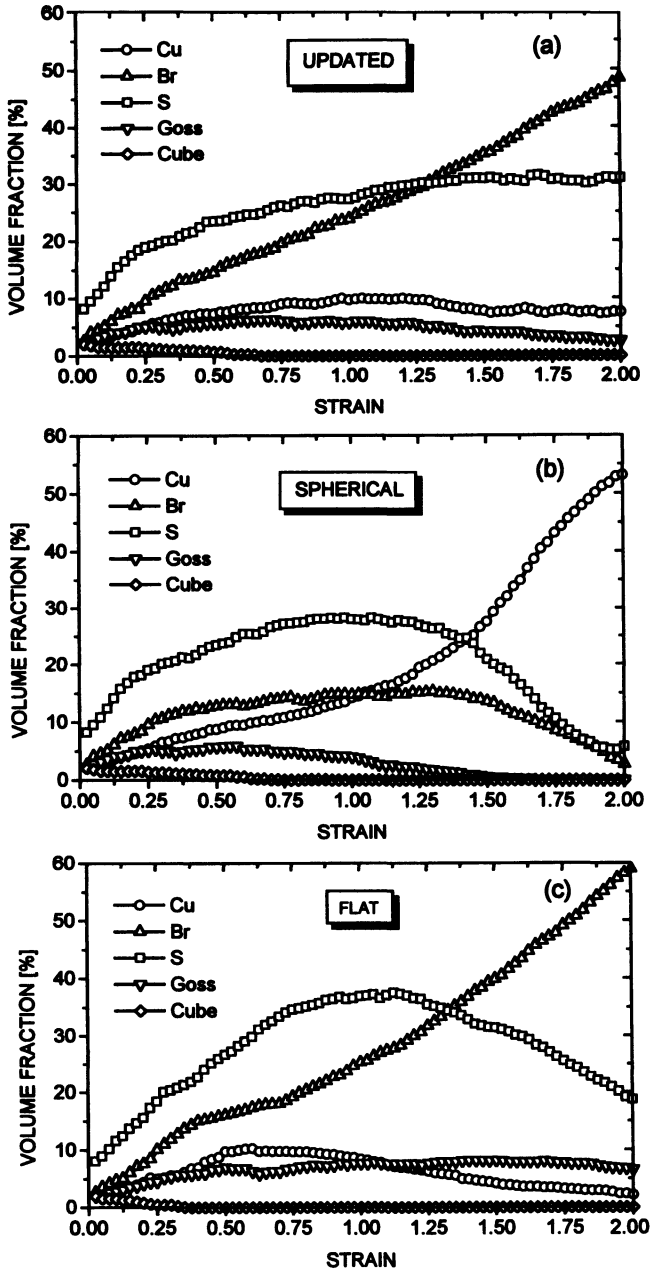


FIGURE 4 Development with strain of the five main texture components: (a) for updating of the grain shape; (b) for permanently spherical grains; (c) for permanently flat grains.

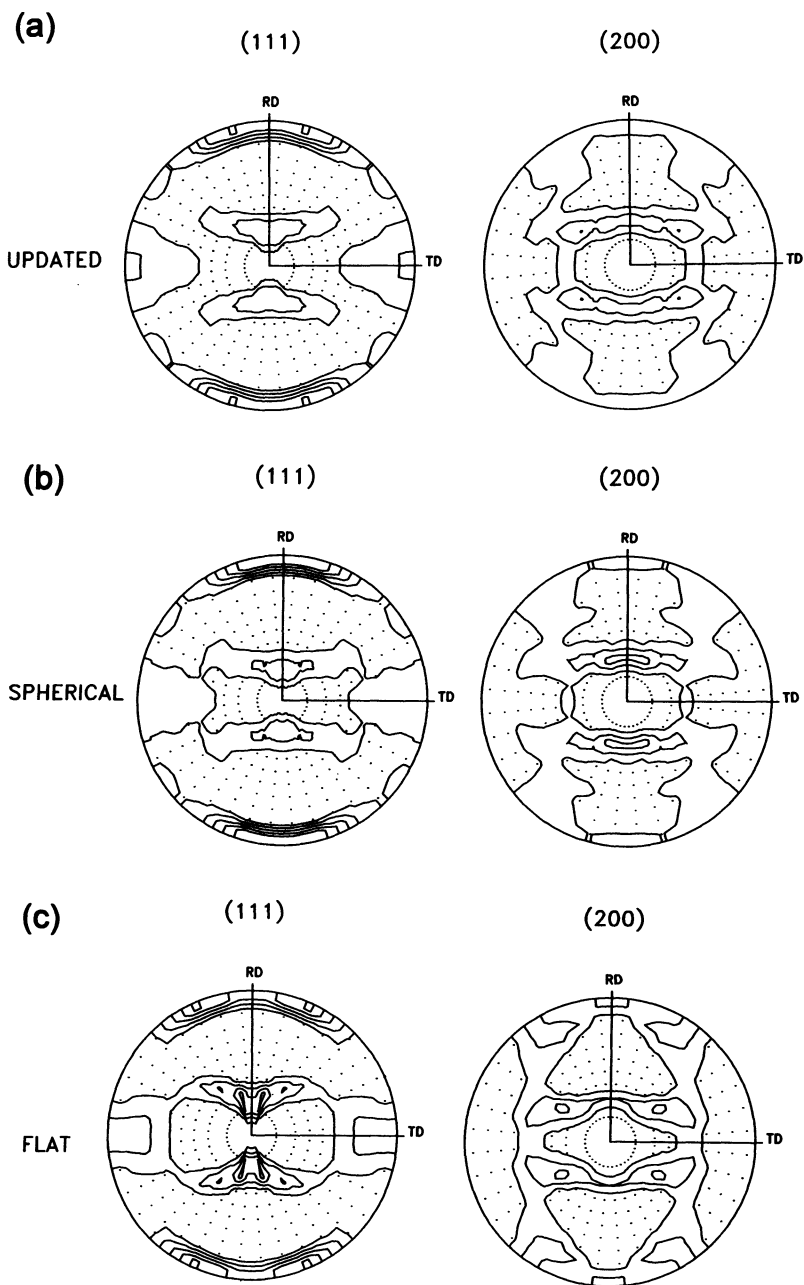


FIGURE 5 $\{111\}$ and $\{200\}$ calculated pole figures (in equal area projection) for a von Mises equivalent strain of 0.5. Dotted areas are below random pole density, and the contour lines represent 1, 2, 3, 4 and 5 times random pole density: (a) for updating of the grain shape; (b) for permanently spherical grains; (c) for permanently flat grains.

DISCUSSION

It is an integral part of the present VPSC scheme that the initial lattice rotation rule is MA and that the rule changes with increasing deviation from equiaxed grain shape. The present work has shown that the change is towards PSA – a rule formulated completely independently of the VPSC scheme. This must be seen as a joint support for the VPSC scheme and the PSA concept.

For the specific case dealt with – the maximum deviation of the strain in the individual grains from the macroscopic strain which the VPSC program can provide – we perform an objectively based transition from MA to PSA. It should be noticed that there is not a one-to-one correspondence between the MA to PSA transition as monitored by the indicators in Figs. 2 and 3 and the MA to PSA transition in the texture development. As judged from the incremental indicators, the transition is halfway through at a strain of ~ 0.5 . For updating one would therefore expect the texture after a strain of 0.5 to be dominated by MA (the strain range up to 0.5 starts with pure MA rules and ends halfway between MA and PSA rules). As a matter of fact the pole figures are much closer to those for flat grains (PSA) than to those for spherical grains (MA). For the copper component updating even leads to a volume fraction outside the range defined by pure MA and pure PSA.

The importance of the whole problem of the lattice rotation rules obviously depends on the occurrence of local deviations from the macroscopic strain. There is an increasing awareness that such deviations, deviations from the full-constraint Taylor model (Taylor, 1938), do occur for a number of reasons (for a recent general discussion see Van Houtte (1996)). The deviations may be dictated by the microstructure or the phase structure (e.g. Leffers, 1996; Bolmaro *et al.*, 1997; Lebensohn and Canova, 1997; Christoffersen and Leffers, 1997). With the VPSC model even single-phase materials without an extreme n value as in the present work show very significant deviations from the full-constraint Taylor model (e.g. Molinari *et al.*, 1987). Finite-element modelling provides a very direct theoretical proof of local deviations from the macroscopic strain, e.g. the FEM work on rolled iron by Dawson *et al.* (1994) and the FEM work on rolled copper by Mika and Dawson (1998). And of course there are strain deviations in the relaxed-constraint model in any of its variants – linked to grain shape

or in the recent formulation without direct link to grain shape by Van Houtte (1995).

The actual texture development under the imposed Sachs-like conditions (imposed by a very low degree of rate sensitivity) confirm the results of Leffers and Lebensohn (1996), including the surprising observation that Sachs-type deformation with MA lattice rotation (permanently spherical grains) leads to a copper-type texture. For the simple Sachs model Leffers and Lebensohn found a texture with the copper component as the one predominant texture component already at 50% rolling reduction, corresponding to a von Mises equivalent strain of 0.78. In the present work considerably higher strains (strains > 1.5) are required to get such a predominance of the copper component. We refer this difference to the fact that even with $n = 47$ the present model does not really reach proper Sachs conditions. Using the modified Sachs model (Pedersen and Leffers, 1987), which also deviates from the rigorous Sachs model, Leffers and Lebensohn found a multicomponent copper-type texture at 50% reduction.

As our final remark we want to state that the updating scheme is based on the assumption that one may consider an elongated and flattened grain as a homogeneously deforming entity (an assumption which is an integral part of the great majority of polycrystal models, including all variants of the Taylor and the Sachs model). This is not necessarily correct; a flat grain may split up into approximately equiaxed crystallites with their individual deformation and rotation patterns (e.g. Mika and Dawson, 1998). Actually, the microstructural conditions may determine whether the grains maintain their identity or split up. One might imagine that the twinned/bundled grains in materials developing the brass-type texture (Duggan *et al.*, 1978; Leffers, 1996; Christoffersen and Leffers, 1997) maintain their identity, thus enforcing updating, while the grains in materials developing the copper-type texture (without identity conserving twins) split up, thus effectively remaining equiaxed. This could provide a completely new explanation for the fcc rolling-texture transition.

CONCLUSION

The viscoplastic self-consistent model leads to a transition from MA lattice rotation to PSA lattice rotation with increasing deviation from

equiaxed grain shape. The textures resulting from MA and PSA are quite different.

Acknowledgement

This work was partially carried out within the Engineering Science Centre for Structural Characterization and Modelling of Materials at Risø. The authors are grateful for the support from the Fundacion Antorchas. The authors want to thank D.P. Mika and P.R. Dawson for access to their unpublished work.

References

- Bolmaro, R.E., Lebensohn, R.A. and Brokmeier, H.-G. (1997). *Comp. Mater. Sci.*, **9**, 237.
- Christoffersen, H. and Leffers, T. (1997). *Scripta Mater.*, **37**, 1429.
- Dawson, P.R., Beaudoin, A.D. and Mathur, K.K. (1994). *Numerical Prediction of Deformation Processes and the Behaviour of Real Materials*. Andersen, S.I. et al. (Eds.) Risø National Laboratory, Roskilde, p. 33.
- Duggan, B.J., Hatherly, M., Hutchinson, W.B. and Wakefield, P.T. (1978). *Mater. Sci.*, **12**, 343.
- Hosford, W.F. (1977). *Text. Cryst. Solids*, **2**, 175.
- Kocks, U.F. and Chandra, H. (1982). *Acta Metall.*, **30**, 695.
- Kocks, U.F., Tomé, C.N. and Wenk, H.-R. (1998). *Texture and Anisotropy*. Cambridge University Press, Cambridge, pp. 326–389.
- Lebensohn, R.A. and Canova, G.R. (1997). *Acta Mater.*, **45**, 3687.
- Lebensohn, R.A. and Tomé, C.N. (1993). *Acta Metall. Mater.*, **41**, 2611.
- Leffers, T. (1994). *Materials Science Forum*, **157–162**, 1815.
- Leffers, T. (1996). *Proceedings ICOTOM 11*. Liang, Z. et al. (Eds.) International Academic Publishers, Beijing, p. 299.
- Leffers, T., Asaro, R.J., Driver, J.H., Kocks, U.F., Mecking, H., Tomé, C. and Van Houtte, P. (1988). *Proceedings ICOTOM 8*. Kallend, J.S. and Gottstein, G. (Eds.) The Metallurgical Society, Warrendale, p. 265.
- Leffers, T. and Lebensohn, R.A. (1996). *Proceedings ICOTOM 11*. Liang, Z. et al. (Eds.) International Academic Publishers, Beijing, p. 307.
- Mika, D.P. and Dawson, P.R. (1998). *Mater. Sci. Eng. A*, **257**, 62.
- Molinari, A., Canova, G.R. and Ahzi, S. (1987). *Acta Metall.*, **35**, 2983.
- Pedersen, O.B. and Leffers, T. (1987). *Constitutive Relations and Their Physical Basis*. Andersen, S.I. et al. (Eds.) Risø National Laboratory, Roskilde, p. 147.
- Sachs, G. (1928). *Z. verein. deut. Ing.*, **72**, 155.
- Taylor, G.I. (1938). *J. Inst. Metals*, **62**, 307.
- Tiem, S., Berveiller, M. and Canova, G.R. (1986). *Acta Metall.*, **34**, 2139.
- Van Houtte, P. (1981). *Proceedings ICOTOM 6*. Nagashima, S. (Ed.) The Iron and Steel Institute of Japan, Tokyo, p. 428.
- Van Houtte, P. (1995). *Acta Metall. Mater.*, **43**, 2859.
- Van Houtte, P. (1996). *Proceedings ICOTOM 11*. Liang, Z. et al. (Eds.) International Academic Publishers, Beijing, p. 236.